
Article:
Lu, Q., Zhou, X., Krysa, A. orcid.org/0000-0001-8320-7354 et al. (4 more authors) (2018) InAs thermophotovoltaic cells with high quantum efficiency for waste heat recovery applications below 1000 degrees C. Solar Energy Materials and Solar Cells, 179. pp. 334-338. ISSN 0927-0248

https://doi.org/10.1016/j.solmat.2017.12.031

InAs thermophotovoltaic cells with high quantum efficiency for waste heat recovery applications below 1000 °C

Qi Lu[a,*], Xinxin Zhou[b], Andrey Krysa[b], Andrew Marshall[a], Peter Carrington[c], Chee-Hing Tan[b] and Anthony Krier[a]

[a] Physics department, Lancaster University, Lancaster, LA1 4YB, United Kingdom

[b] Department of Electronic and Electrical Engineering, University of Sheffield, Sheffield, S3 7HQ, United Kingdom

[c] Engineering department, Lancaster University, Lancaster, LA1 4YW, United Kingdom

* Corresponding author. E-mail address: q.lu3@lancaster.ac.uk

InAs thermophotovoltaic (TPV) cells with external quantum efficiency at the peak wavelengths reaching 71% at low temperature and 55% at room temperature are reported, which are the highest values to date for InAs. The TPV exhibited 10% power conversion efficiency at 100 K cell temperature. The dark and light current-voltage characteristics were measured at different cell temperatures (100-340 K) in response to heat sources in the range 500-800 °C. The resulting dependences of the output voltage and current as well as the spectral response of the InAs TPV have been extensively characterized for waste heat recovery applications. The performance of these cells is strongly determined by the dark current which increases rapidly with increasing cell temperature originating from bandgap narrowing, which resulted in a reduction of open circuit voltage and output power.

Key words:

Thermophotovoltaics; indium arsenide; waste heat recovery; quantum efficiency

1. Introduction

Large amounts of energy are lost in the form of waste heat in high energy consumption industries such as glass and steel manufacturing. In some processes as much as 20-50% of the waste heat can be lost as radiation. Clearly, a direct and convenient way of converting waste heat into electricity is highly desirable. TPV cells which have very similar operating principles to solar cells can absorb the radiation from hot sources and produce electricity [1]. In addition to energy scavenging, TPVs also have potentials for use in a wide variety of other applications including automotive, mobile power generation and military power supplies and also for space applications where TPVs operating at low temperature can be employed using passive cooling.

Until recently, research work on TPVs has been focused on silicon [2], InGaAs [3], GaSb [4,5] and GaInAsSb alloys lattice matched on GaSb [6,7], most of which have a relatively wider bandgap, making them more suitable for electricity generation from heat sources at temperatures above 1000 °C. Among these, excellent performance has been reported from GaInAsSb TPVs lattice matched on GaSb substrates [6]. Such devices can produce an open circuit voltage (V_{oc}) of ~0.3 V, a short circuit current density (J_{sc}) up to 3 A/cm^2, and about 90% internal quantum efficiency (IQE) [8,9]. For higher temperature sources, GaSb based TPVs can achieve ~16% power conversion efficiency provided they are illuminated by a high intensity (tungsten) light source [10]. However, for lower temperature (< 1000 °C) heat sources, narrow bandgap semiconductors can potentially result in TPVs with higher conversion efficiency [11,12], mainly because more photons emitted from the blackbody source can be harvested by the low bandgap material. InAs TPV cells (0.35 eV bandgap) appear to be very promising for waste heat recovery. However, until now, much less investigation has been carried out on InAs based TPVs compared with GaInAsSb and GaSb devices. V_{oc} of ~0.06 V and J_{sc} of ~0.9 A/cm^2 have been obtained from InAs TPV cells illuminated by a 950 °C thermal source [13]. But relatively little information has been reported on the operating characteristics and potential of InAs TPVs. In this work, we report in detail on the characteristics of a TPV cell based on a high quality InAs p-i-n diode grown by metal-organic chemical vapor deposition (MOCVD) for the purpose of waste heat recovery and energy scavenging applications. We report on the electrical and spectral properties for the cell held at different temperatures (100- 340 K) when illuminated by low temperature thermal sources (500-1000 ^{o}C). We obtained high external quantum efficiency (EQE), short circuit current and approximately 3.6% power conversion efficiency using a 950 °C thermal source.

2. Experiments

The InAs p-i-n TPV devices studied in this work were grown by MOCVD on an n-type InAs (100) substrate. The structure comprised of a 2 μm n+ layer (1×10^{18} cm^{-3}) followed by an 10 μm intrinsic region and then a 2 μm p+ layer (1×10^{18} cm^{-3}). Ti/Au metal with thickness of 20/200 nm was

deposited to form the top and bottom ohmic contacts. The top contact was in a horseshoe shape covering 20% of the surface area as shown in the inset of Fig. 1, which was opaque for the incident radiation. The TPV cells were fabricated by using phosphoric acid and hydrogen peroxide based wet chemical etchant, followed by a finishing etch in sulphuric acid and hydrogen peroxide based solution, to define mesa diodes with diameter of 400 µm. A scanning electron microscopic (SEM) image was taken on the etched device, as shown in Fig. 1. The deep wet etching resulted in the extension of the side walls by about 8 µm, making the actual diameter to be around 416 µm. The finished devices were mounted on TO- headers for characterization.

The current-voltage (I-V) characteristics were measured using a Keithley 2400 source meter. Flash exposure tests were carried out by mounting the cells 10 cm in front of a variable temperature (500-800 °C) blackbody thermal source with an aperture of 25 mm, without any focusing optics. The TPV device was loaded into a liquid nitrogen cooled continuous flow cryostat to measure the I-V characteristics and spectral response at different cell temperatures (T_c). The corresponding spectral response was measured using the same black body source, with a 0.3 m grating monochromator (blazed at 3.5 µm) and lock-in amplifier with a chopper frequency of 65 Hz. The EQE curves were obtained by dividing the spectral responses with the spectrum of the thermal source, which was measured by using a pyroelectric infrared detector. The EQE value of the cell at 300 K 1.55 µm was measured outside of the cryostat by using a 1.55 µm, 1mW fiber pigtailed laser. The values of the EQE curves were then scaled based on this measured EQE.

3. Results and discussion

The capacitance-voltage (C-V) measurements reported previously revealed a very low background n-doping level of $6x10^{14}$ /cm^3 in the intrinsic InAs region [14], which indicated that in the p-i-n structure the depletion region occupied the entire i-region. The top p+ layer can work as the emitter region, and the intrinsically n type undoped region can serve as the base for the InAs TPV. The I-V curves of the InAs cell under 500-800 °C thermal source radiations at cell temperatures T_c = 300 K and 100 K are plotted in Fig. 2 (a) and (b). The measurements were carried out when the InAs cell was mounted in the cryostat with a CaF_2 window in front. The power density from the thermal radiation arriving on the cell was measured using a calibrated power meter to increase from 76 mW/cm^2 at 500 °C to 318 mW/cm^2 at 800 °C. As shown in Fig. 2(a), when the InAs TPV cell was kept at 300 K, the I-V curves remained almost linear regardless of the source temperature, corresponding to a fill factor (FF) of 25%. As the source temperature was increased from 500 °C to 800 °C, the short circuit current, I_{sc} increased from 0.04 mA (0.03 A/cm^2) to 0.29 mA (0.23 A/cm^2), almost proportional to the increase in the number of photons from the black body source above the InAs bandgap energy (~0.35 eV). The V_{oc} also increased from 5.5 mV to 17.4 mV. In contrast, when the cell temperature, T_c was cooled to 100 K, (Fig. 2(b)) the FF substantially improved to 68.5% with the source at 500 °C and reached 70.2%

with the source at 800 °C. Although the I_{sc} was reduced by about 31% due to the increase in the bandgap of InAs at 100 K (~0.41 eV), the V_{oc} significantly improved to 252 mV with the source at 800 °C - more than 14 times larger than at T_c = 300 K. It is also worth noting that the V_{oc} showed much less reduction when lowering the source temperature at T_c = 100 K. With the 500 °C source, the V_{oc} still reached 208 mV, which was only an 18% reduction compared with the 800 °C source. The calculated power efficiency was 0.071 % with the 500 °C source and 0.35% with the 800 °C source when the InAs TPV was at room temperature. However, both values greatly increased to 4.4% and 10% respectively at T_c =100 K, which was predominantly due to the improvement in V_{oc}. These high power conversion efficiencies at low T_c can possibly make the InAs based TPVs useful in deep space applications, where other sources of energy are not available. Note that the incident power in these experiments is quite low (76 mW/cm^2 at 500 °C and 318 mW/cm^2 at 800 °C) since the TPV cell was inside the cryostat, and that the power conversion efficiency is strongly dependent on both the incident power density and the blackbody emitter temperature. When concentrating the 800 °C radiation to about 4 W/ cm^2 at room temperature, the TPV efficiency increased to 1.3%, largely due to the 3 times increase in V_{oc}. Using a 950 °C blackbody source with 720 mW/cm^2 power density as in our previous work, this InAs TPV achieved J_{sc} = 1.32 A/cm^2 at 300 K T_c, which is about 47% higher than the LPE grown InAs TPV with an InAsSbP window layer [13]. The power efficiency was estimated around 3.6%, which is also a little higher than our previously reported value.

The spectral responses of the InAs TPV at these two cell temperatures were shown in Fig. 2(c) and (d). In each case, the shape of the response showed very slight changes by varying source temperature. Only the intensity was increased with higher source temperatures due to more photons above the bandgap energy being captured. The small fluctuations in the spectra in the 1.6-1.8 µm and 2.5-2.8 µm regions were caused by the water absorption in the atmosphere. The spectra in Fig. 2(d) all showed a clear cut-off once the wavelength was above 3.0 µm, indicating that very little absorption occurred below the InAs bandgap when the TPV cell was at 100 K. In contrast, at T_c =300 K in Fig. 2(c), much broader tails can be observed in all the spectra between 3.5 and 4.0 µm, which can be attributed to the absorption by thermally activated near band edge states. In addition, by comparing these two plots, it is clear that at 300 K the InAs TPV cell exhibited a broader spectral response, while at 100 K the curves became narrower and clear peaks can be observed near the InAs bandgap.

The dark current density-voltage (J-V) curves of the InAs TPV were measured when the TPV cell temperature, T_c was adjusted from 100 K up to 340 K, as shown in Fig. 3(a). The estimated ideality factor n remained at around 1.1 in the measured temperature range. The dark leakage current density J_0 greatly increased by about 4 orders of magnitude when T_c was raised from 100 K to 340 K. We found that the dark current did not drop significantly at temperatures below 100 K. Using an additional metal cap made of 0.2 mm thick nickel which can block all the possible infrared light from the environment, the dark current drops substantially (by at least 2 orders of magnitude), indicating

that the device is collecting the 300 K radiation from the optical window of cryostat. Hence, the dark current at 100 K is believed to be largely contributed by the 300 K radiation.

The shunt resistance R_0 of the InAs TPV at different temperatures was estimated from these dark J-V curves near zero bias. The relation between R_0A and T_c is illustrated in Fig. 3(b), where A denotes the actual area of the TPV. From this graph, three distinct regions can be identified, as illustrated by the straight lines on the plot. For T_c<140 K, the R_0A value was almost independent of the cell temperature, indicating that the 300 K background induced current was the dominant contributions to the dark current. For 140 K<T_c<240 K the slope of the fit was about half of that for the region T_c>240 K, which suggests that generation-recombination (G-R) played a major role in the dark current for 140 K<T_c<240 K, and diffusion current was the most important contribution for T_c>240 K.

Complete T_c dependent characterization of the InAs TPV performance was carried out between 100 K and 340 K under the illumination from an 800 °C thermal source at 318 mW/cm^2 power intensity. Fig. 4(a) depicts the I-V characteristics under these conditions. The FF gradually degraded from 70% at 100 K to 33% at 280 K, and stayed constant at around 25% above 280 K. The I_{sc} and V_{oc} at each temperature taken from this graph are plotted in Fig. 4(b). With increasing T_c, the I_{sc} slowly increased from 0.2 mA at 100 K to about 0.3 mA at 340 K, which is in very good agreement with the narrowing of InAs bandgap with increasing temperature. Using the Varshni relation the InAs bandgap reduces from 0.40 eV at 100 K to 0.34 eV at 340 K, corresponding to a 48% increase in the number of incident photons with above bandgap energy. In contrast however, the V_{oc} dramatically dropped from 252 mV at 100 K to 3.8 mV at 340 K, which was the main reason for the large drop of more than 100 times in TPV output power, as shown in Fig. 4(c). Moreover, it can be noticed from Fig. 4(c) that the drop in output power accelerated for T_c above 240 K. As discussed before, this was also the region where diffusion current became the dominant dark conduction current mechanism, resulting in much quicker rise of J_0 in this temperature range as shown in Fig. 4(a). The high J_0 became the main factor determining the low V_{oc} and low output power from the InAs TPV cell in the high T_c regime, which largely originated from the narrow bandgap of InAs. The exponential increase of J_0 when reducing the material bandgap has been presented in [6,7]. For the more mature GaInAsSb TPV technology, a wide bandgap AlGaAsSb layer and a GaSb window layer were often incorporated in the structure to achieve better performance [7]. Such elements will need to be included in the InAs TPV design to improve V_{oc} and the power efficiency in the future.

The EQE curves for the InAs TPV cell at different T_c were extracted from the measured spectral responses using the 800 °C thermal source and are plotted in Fig. 5(a). (The fluctuations in the 1.6-1.8 µm and 2.6-2.8 µm regions were caused by the water absorptions in atmosphere). Similar to the observations from Fig. 2(c) and (d), with higher T_c, the EQE spectra extended much more below the InAs bandgap. The EQE at 300 K mainly fell within the range 0.5-0.6, averaging about 0.55. Using a

laser at 1550 nm incident on the TPV cell placed outside the cryostat, we measured a responsivity of 0.79 A/W, corresponding to an EQE of 0.63, which is the highest room temperature EQE reported from InAs based TPVs. Despite its much narrower bandgap, this EQE value is as good as the highest EQE reported from GaSb and GaInAsSb based TPV cells (~60%) [4,6]. With improved structural design such as depositing an anti-reflection coating on top, it is likely that the EQE from InAs TPVs can be further enhanced.

At different T_c, the peak EQE values close to the cut-off wavelengths were taken from these spectra and were plotted in Fig. 5(b) (red dots). At low temperatures, the EQE reached a maximum value of 0.71, which was very near the theoretical maximum value (about 30% of the efficiency was lost due to surface reflection – no antireflection coating was applied to our cells). One interesting observation from the EQE spectra was that at shorter wavelengths the EQE first increased, then decreased with rising T_c. For example, the EQE at 2.0 µm was plotted in Fig. 5(b) for comparison. The different trends between these two curves might be caused by different absorption profiles within the InAs TPV. For photons with close to the bandgap energy (red dots), the smaller absorption coefficient ($\alpha \sim 10^3$ cm^{-1} range) results in the photons penetrating the full depth of the InAs i-region. The photo-excited minority carrier (holes) need to transit across the entire depletion region to be collected by the contacts resulting in some reduction of EQE near the cut-off wavelength at higher T_c. One key factor determining this is the carrier lifetime. Previously it has been analyzed that in InAs LEDs, non-radiative Auger recombination is the main reason for the reduced LED efficiency [15]. Similarly, in the InAs TPV cell, the stronger Auger process at higher T_c would significantly decrease the carrier lifetime, thus reducing the collection efficiency. In contrast, for higher energy photons (blue dots), α becomes much larger ($\sim 10^4$ cm^{-1}). These photons would be absorbed mostly in top part of the depletion region. The photo-generated holes can be more easily collected due to their proximity to the p-contact. The temperature dependence of the EQE in this wavelength range is still not fully understood. Possible reasons might be the surface recombination mechanisms in the top p-InAs region, which could consume some of the carriers excited by higher energy photons.

4. Conclusion

We have systematically characterized the performance of InAs TPV cells with low temperature thermal sources at different cell temperatures T_c. It has been found that T_c has a huge impact on the J_{sc}, V_{oc} and output power from the InAs cell. The power conversion efficiency increased by about 28 times with an 800 °C source when the cell was cooled from 300 K to 100 K, mostly because of the significant enhancement of V_{oc} at lower T_c. At 100 K T_c, 10% power conversion efficiency has been reported, which can make the InAs based TPVs a promising power source for deep space applications. Under the same illumination conditions, the I_{sc} from the InAs TPV gradually increased by about 50% when the cell temperature was raised from 100 K to 340 K, largely due to the InAs bandgap

narrowing. However, the V_{oc} significantly decreased from 252 mV to only 3.8 mV, resulting in the output power being reduced by about two orders of magnitude. The quicker reduction of output power at higher temperatures could be related to the faster increase of J_0 in the same temperature range. The EQE from the InAs TPV was determined to be ~55% over most of the sensitive range at room temperature, which is the highest value reported to date for InAs, with no anti-reflection coating. A peak value of 71% was achieved at 140 K. The high EQE was partly caused by the thick MOCVD grown i-region, so that almost all incident photons above the bandgap energy can be absorbed. The change in the EQE spectra with T_c showed some wavelength dependence and the limited hole lifetime is one reason for the reduction of EQE at higher T_c, which needs to be taken into account for the design of future InAs based TPV cells. With further structural improvements such as carrier blocking layers to reduce J_0 at higher T_c, the V_{oc} and output power can be further enhanced. Concentration of the incident radiation at room temperature can also greatly improve V_{oc} and the power efficiency, due to the higher value of I_{sc}.

In addition, the extra wide spectra from lower temperature blackbodies need to be taken into account towards realizing applicable TPVs for waste heat recovery. In these cases, single junction TPVs will inevitably either have huge thermalization loss when using narrow bandgap materials, or only be able to collect a small fraction of the emitted energy when using wide bandgap materials. A multi-junction TPV system is a promising route to achieving the highest possible power efficiency, similar to the case of multi-junction solar cells [16]. With a bandgap of 0.35 eV, an efficient InAs TPV can serve as the intermediate or bottom section in the multi-junction TPV design.

Acknowledgements

Financial support for this work was provided by the EPSRC grant (funding No.: EP/P012035/1). The InAs wafer was partly supported by The University of Sheffield EPRSC IAA Account (EP/K503812/1) to further develop work done under an EPSRC grant (EP/H0131464/1). P.J.C. acknowledges support from the Royal Academy of Engineering and the Joy Welch Educational Charitable Trust. The underlying data in this paper is available from http://dx.doi.org/10.17635/lancaster/researchdata/182.

References

[1] H. Daneshvar, R. Prinja, N.P. Kherani, Thermophotovoltaics: Fundamentals, challenges and prospects, Appl. Energy. 159 (2015) 560–575.

[2] B. Bitnar, W. Durisch, D. Grutzmacher, J.C. Mayor, C. Muller, F. von Roth, J.A.A. Selvan, H. Sigg, H.R. Tschudi, J. Gobrecht, A TPV system with silicon photocells and a selective emitter,

Conf. Rec. IEEE Photovolt. Spec. Conf. (2000) 1218–1221.

[3] M. Tan, L. Ji, Y. Wu, P. Dai, Q. Wang, K. Li, T. Yu, Y. Yu, S. Lu, H. Yang, Investigation of InGaAs thermophotovoltaic cells under blackbody radiation, Appl. Phys. Express. 7 (2014) 96601.

[4] A.W. Bett, O.V. Sulima, GaSb photovoltaic cells for applications in TPV generators, Semicond. Sci. Technol. 18 (2003) S184–S190.

[5] B.C. Juang, R.B. Laghumavarapu, B.J. Foggo, P.J. Simmonds, A. Lin, B. Liang, D.L. Huffaker, GaSb thermophotovoltaic cells grown on GaAs by molecular beam epitaxy using interfacial misfit arrays, Appl. Phys. Lett. 106 (2015) 111101.

[6] M.G. Mauk, V.M. Andreev, GaSb-related materials for TPV cells, Semicond. Sci. Technol. 18 (2003) S191–S201.

[7] M.W. Dashiell, J.F. Beausang, H. Ehsani, G.J. Nichols, D.M. Depoy, L.R. Danielson, P. Talamo, K.D. Rahner, E.J. Brown, S.R. Burger, P.M. Fourspring, W.F. Topper, P.F. Baldasaro, C.A. Wang, R.K. Huang, M.K. Connors, G.W. Turner, Z.A. Shellenbarger, G. Taylor, J. Li, R. Martinelli, D. Donetski, S. Anikeev, G.L. Belenky, S. Luryi, Quaternary InGaAsSb thermophotovoltaic diodes, IEEE Trans. Electron Devices. 53 (2006) 2879–2888.

[8] H.K. Choi, C.A. Wang, G.W. Turner, M.J. Manfra, D.L. Spears, G.W. Charache, L.R. Danielson, D.M. Depoy, High-performance GaInAsSb thermophotovoltaic devices with an AlGaAsSb window, Appl. Phys. Lett. 71 (1997) 3758–3760.

[9] C.A. Wang, H.K. Choi, S.L. Ransom, G.W. Charache, L.R. Danielson, D.M. DePoy, High-quantum-efficiency 0.5 eV GaInAsSb/GaSb thermophotovoltaic devices, Appl. Phys. Lett. 75 (1999) 1305–1307.

[10] T. Schlegl, F. Dimroth, A. Ohm, A.W. Bett, TPV Modules Based On GaSb Structures, AIP Conf. Proc. 738; TPV6 Sixth World Conf. Thermophotovoltaic Gener. Electr. 738 (2004) 285–293.

[11] R.S. Tuley, R.J. Nicholas, Band gap dependent thermophotovoltaic device performance using the InGaAs and InGaAsP material system, J. Appl. Phys. 108 (2010) 084516.

[12] A. Krier, M. Yin, A.R.J. Marshall, S.E. Krier, Low Bandgap InAs-Based Thermophotovoltaic Cells for Heat-Electricity Conversion, J. Electron. Mater. 45 (2016) 2826–2830.

[13] A. Krier, M. Yin, A.R.J. Marshall, M. Kesaria, S.E. Krier, S. McDougall, W. Meredith, A.D. Johnson, J. Inskip, A. Scholes, Low bandgap mid-infrared thermophotovoltaic arrays based on

InAs, Infrared Phys. Technol. 73 (2015) 126–129.

[14] X. Zhou, J.S. Ng, C.H. Tan, InAs photodiode for low temperature sensing, Proc. SPIE 9639, Sensors, Syst. Next-Generation Satell. XIX. 9639 (2015) 96390V.

[15] S.A. Choulis, A. Andreev, M. Merrick, A.R. Adams, B.N. Murdin, A. Krier, V. V. Sherstnev, High-pressure measurements of mid-infrared electroluminescence from InAs light-emitting diodes at 3.3 μm, Appl. Phys. Lett. 82 (2003) 1149–1151.

[16] M.A. Green, Y. Hishikawa, W. Warta, E.D. Dunlop, D.H. Levi, J. Hohl-Ebinger, A.W.H. Ho-Baillie, Solar cell efficiency tables (version 50), Prog. Photovoltaics Res. Appl. 25 (2017) 668–676.

Figure captions

Figure 1. SEM image showing the etched side wall of the InAs TPV. The inset shows the plan view optical microscopic image of the device.

Figure 2. I-V curves of the InAs TPV cell at (a) T_c = 300 K, and (b) T_c = 100 K with varying blackbody source temperatures, and the spectral response plots of the InAs TPV at (c) T_c = 300 K, (d) T_c = 100 K with varying black body source temperatures.

Figure 3. (a) Dark J-V plot of the InAs TPV at different cell temperatures. (b) Resistance area R_0A vs $1000/T_c$ plot of the InAs TPV.

Figure 4. Characteristics of the of the InAs TPV illuminated with an 800 °C thermal source with the device at different cell temperature T_c. (a) I-V curves, (b) short circuit current, I_{sc} (red dots) and open circuit voltage, V_{oc} (blue dots), (c) maximum output power.

Figure 5. (a) The dependence of the EQE at different cell temperatures in response to a black body at 800 °C, (b) the peak EQE near cut-off (red dots) and EQE at 2.0 µm (blue dots).

Figure 1

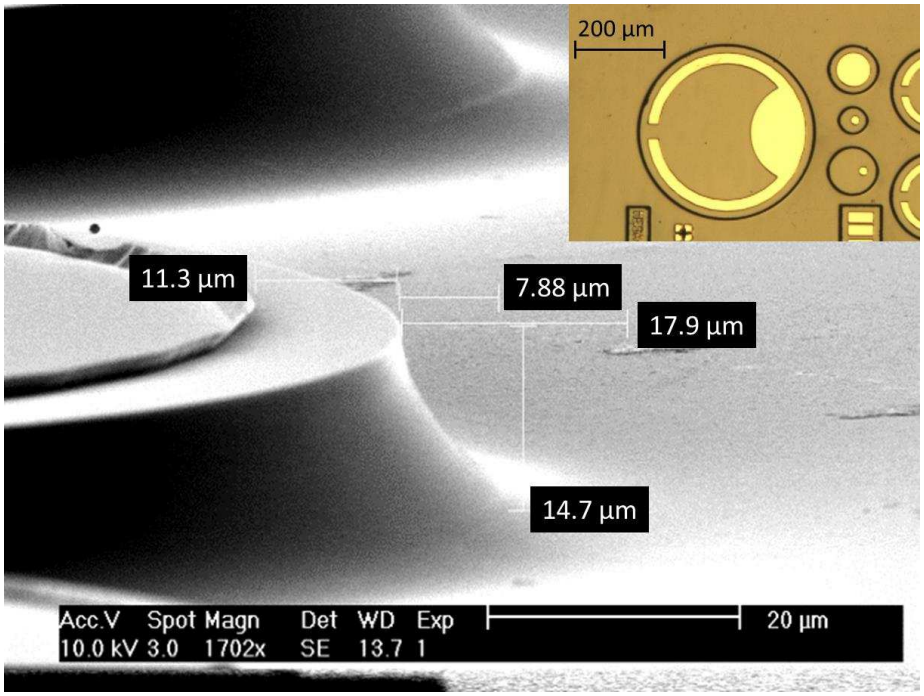

Figure 2(a)

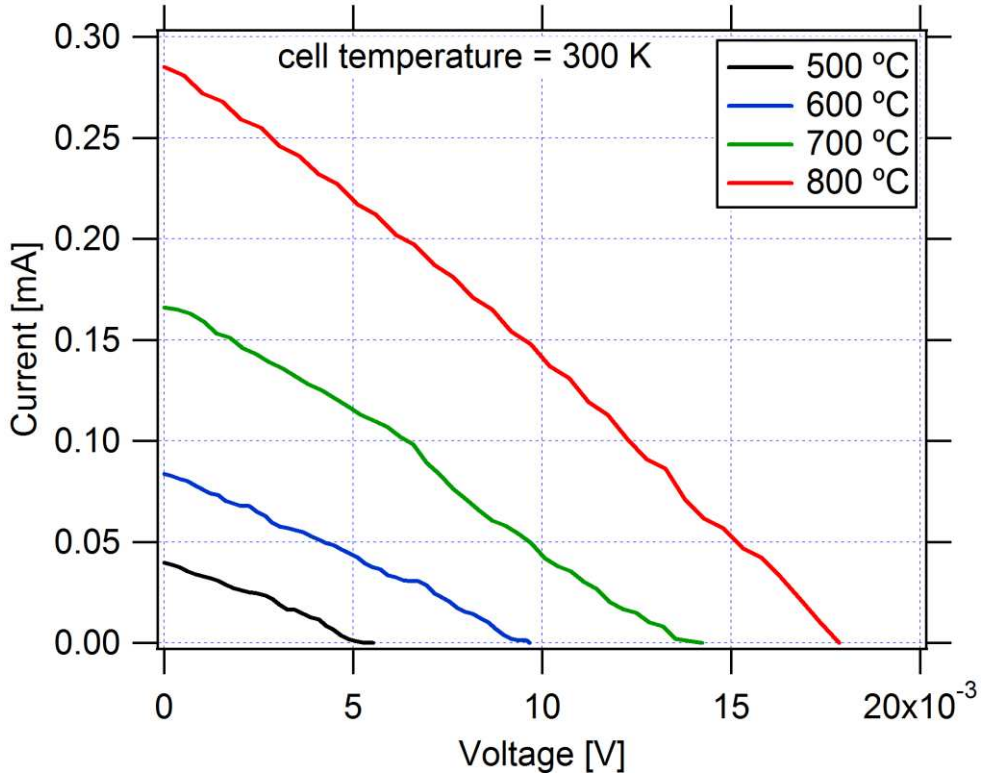

Figure 2(b)

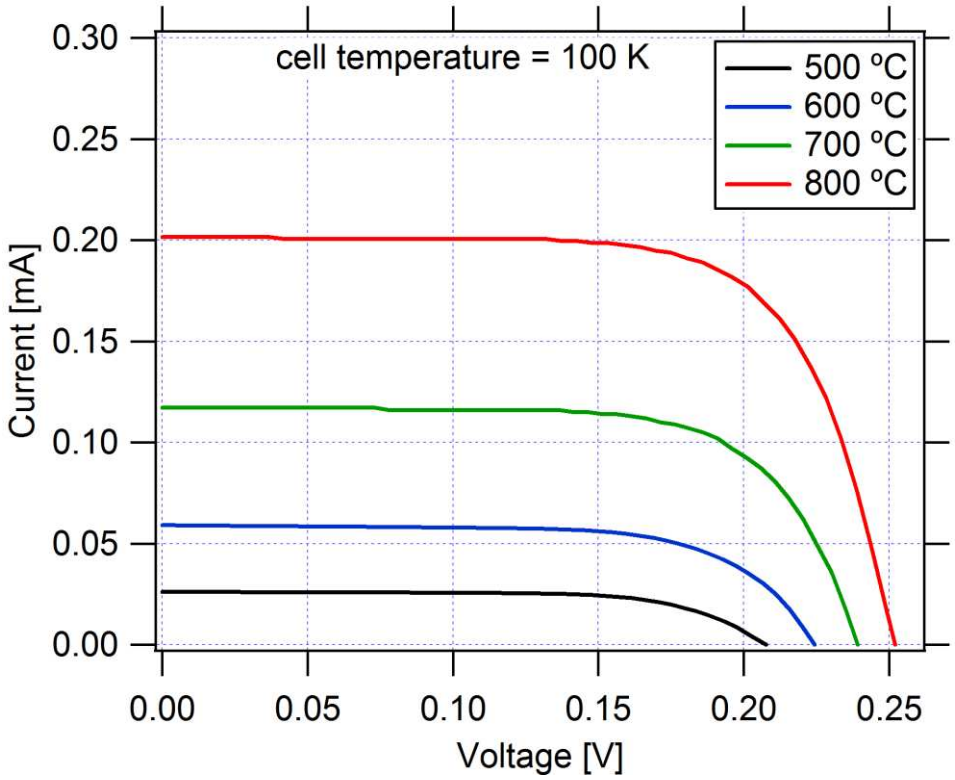

Figure 2(c)

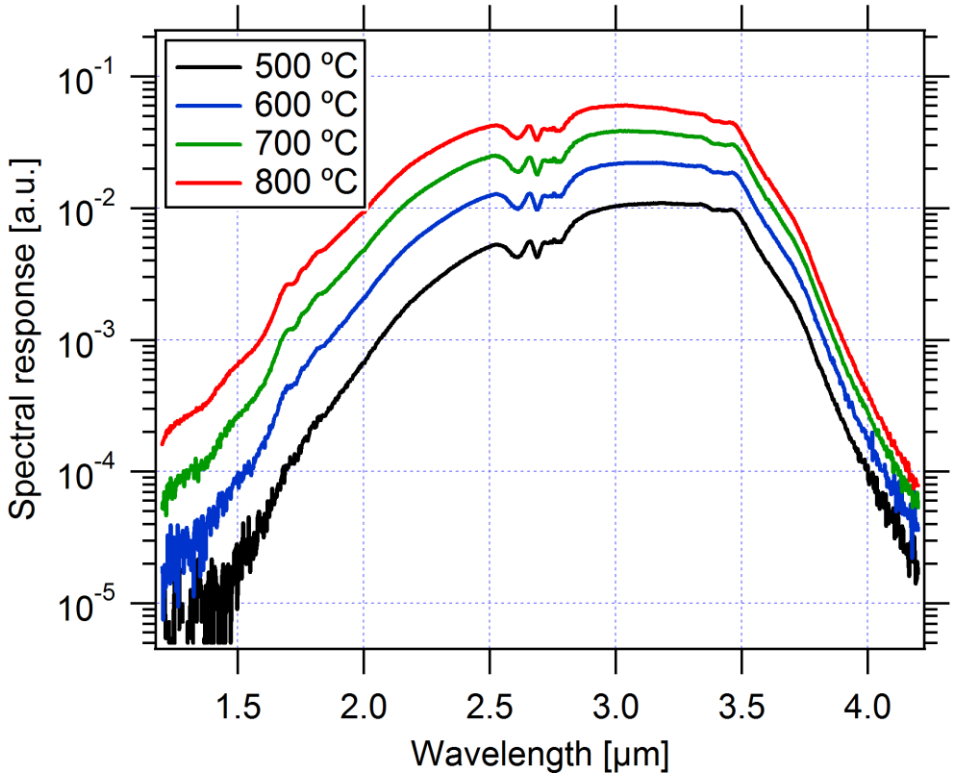

Figure 2(d)

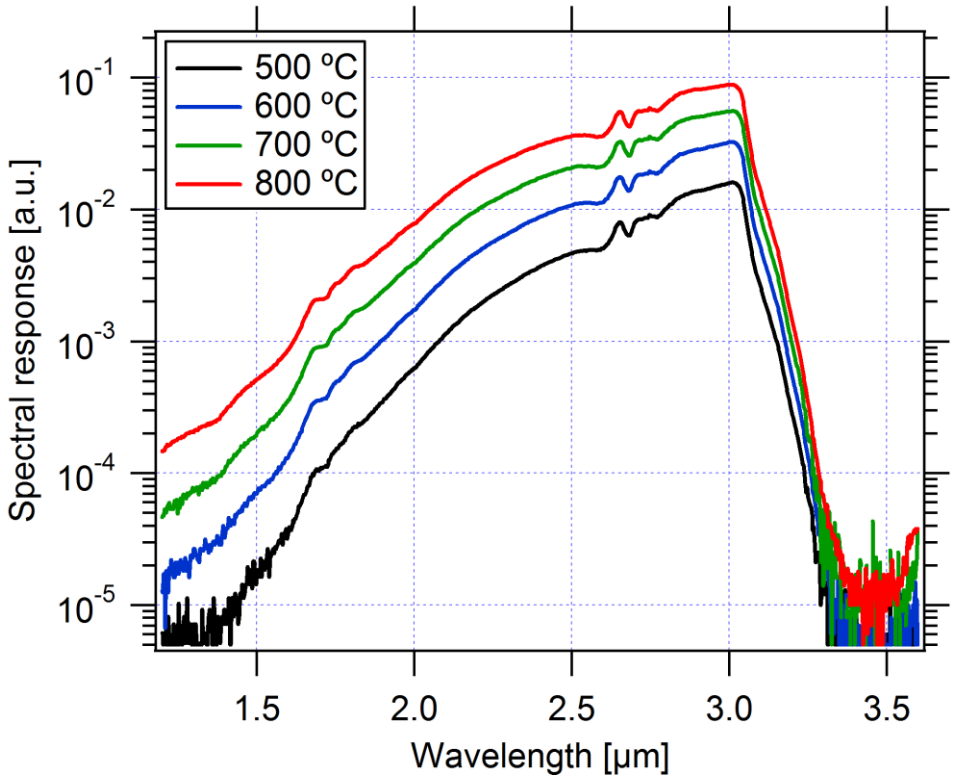

Figure 3(a)

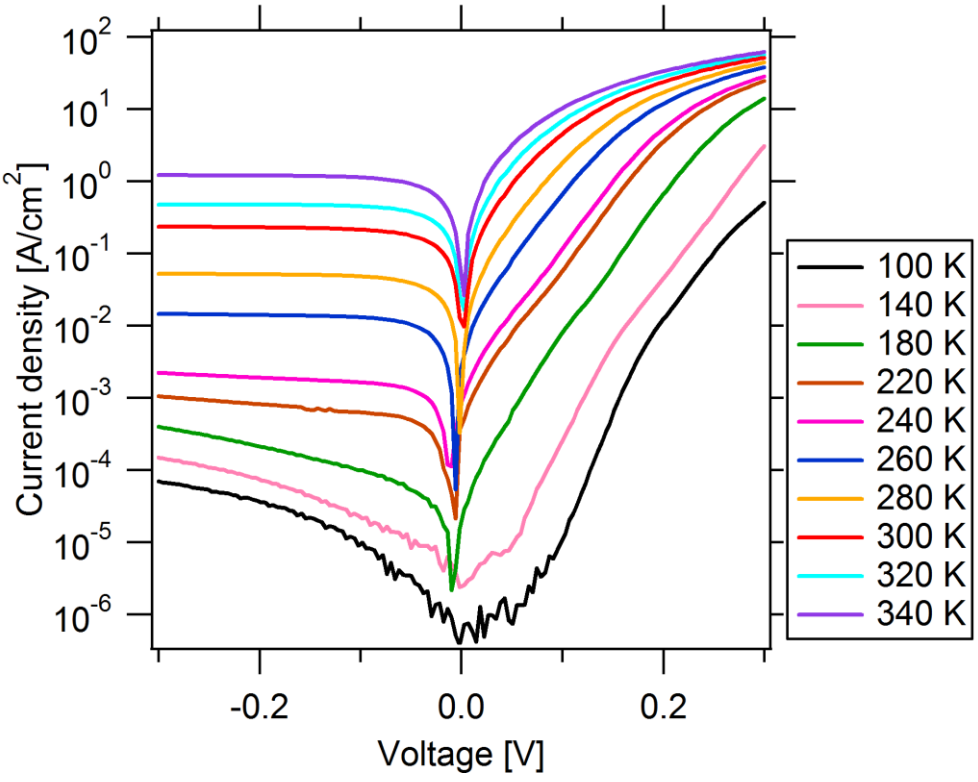

Figure 3(b)

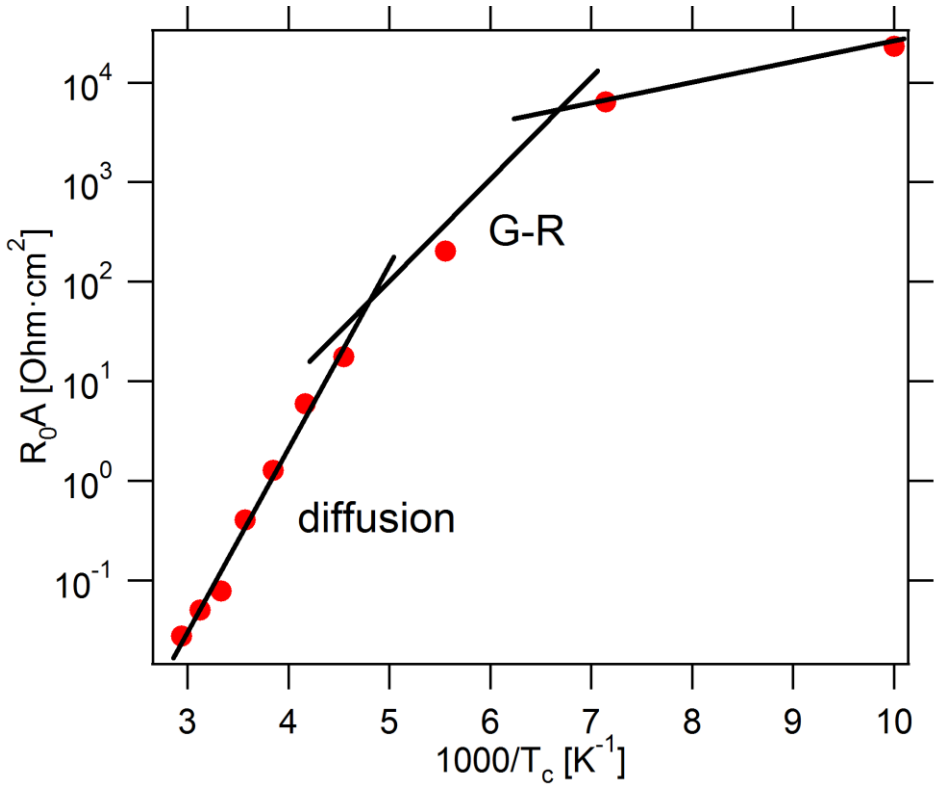

Figure 4(a)

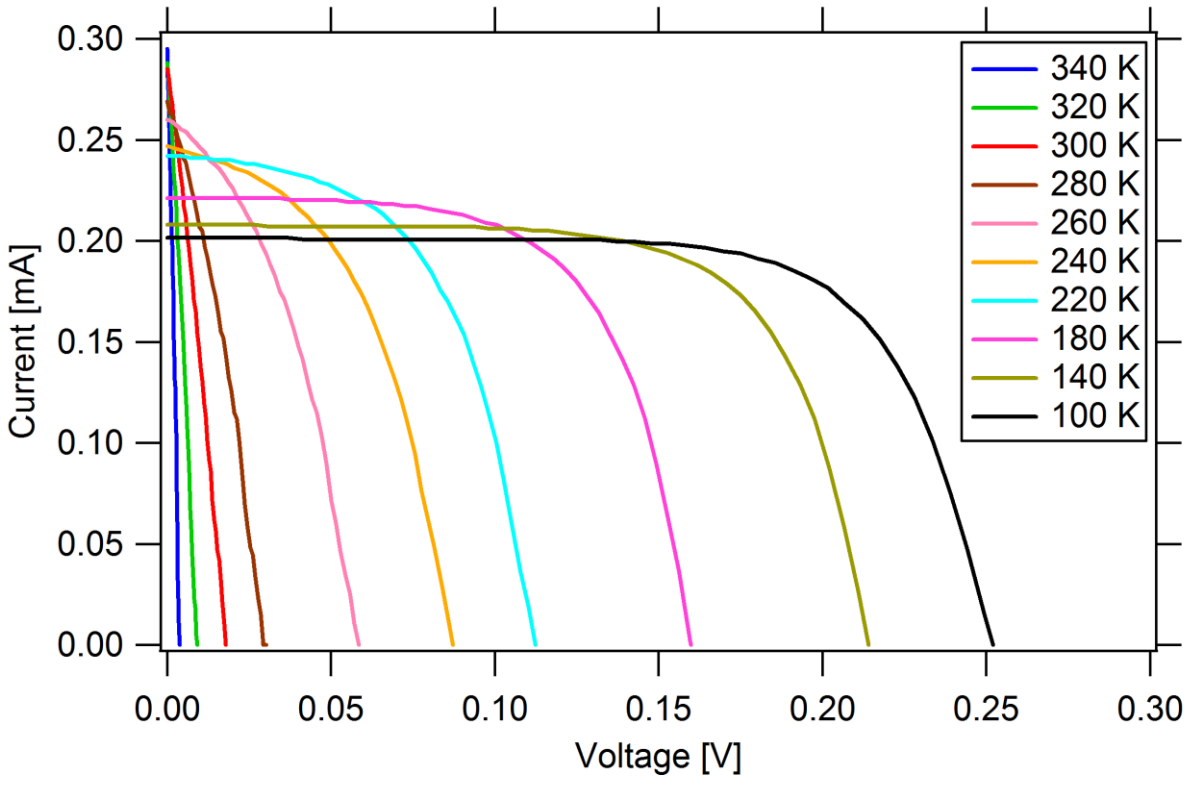

Figure 4(b)

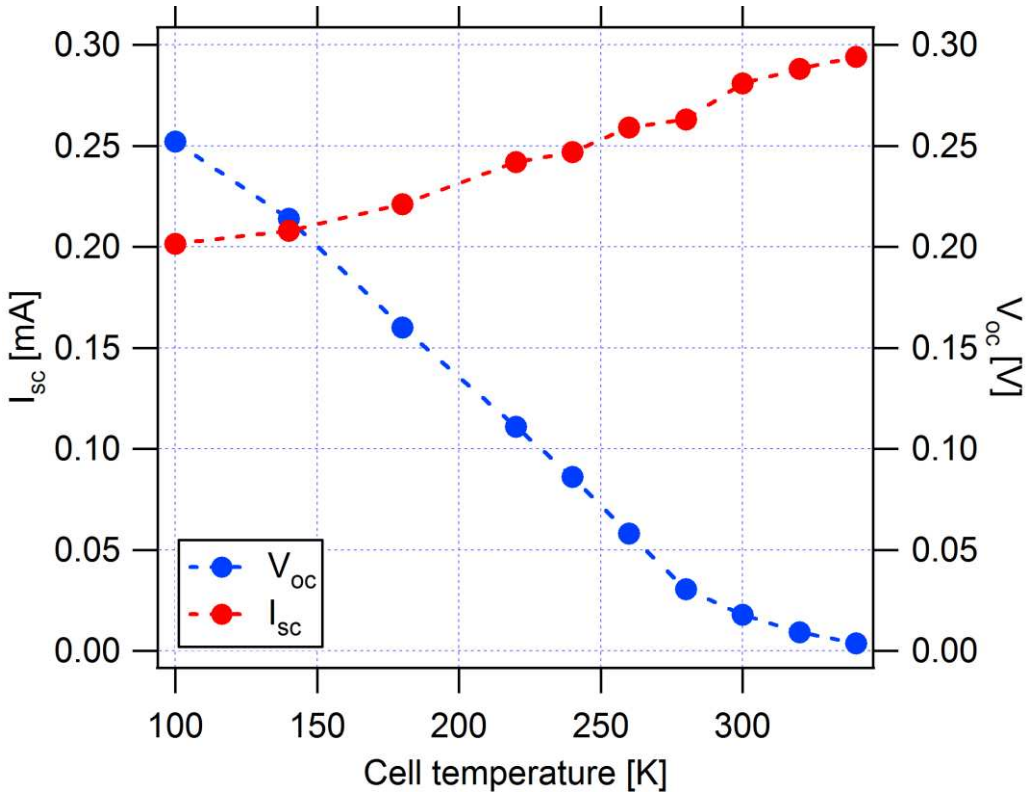

Figure 4(c)

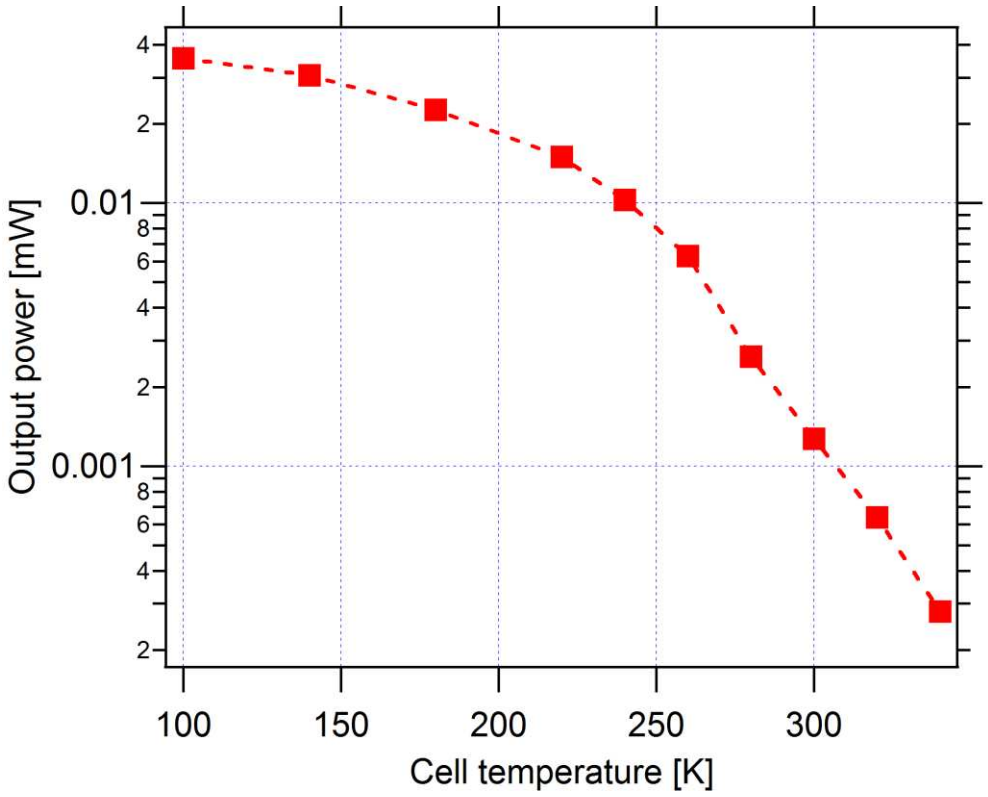

Figure 5(a)

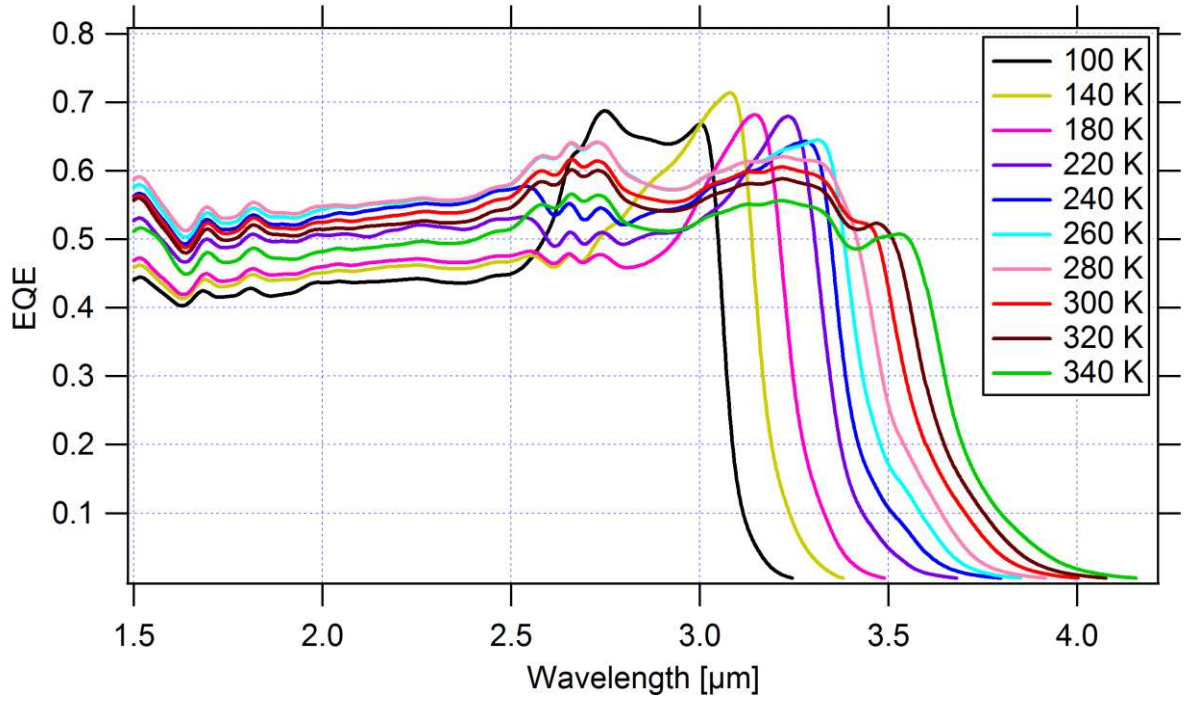

Figure 5(b)